

Thermal neutron captures on d and ${}^3\text{He}$

L. Girlanda^{a,b}, A. Kievsky^b, L.E. Marcucci^{a,b}, S. Pastore^c, R. Schiavilla^{c,d}, and M. Viviani^b

^a*Department of Physics, University of Pisa, 56127 Pisa, Italy*

^b*INFN-Pisa, 56127 Pisa, Italy*

^c*Department of Physics, Old Dominion University, Norfolk, VA 23529, USA*

^d*Jefferson Lab, Newport News, VA 23606*

(Dated: September 4, 2018)

We report on a study of the nd and $n{}^3\text{He}$ radiative captures at thermal neutron energies, using wave functions obtained from either chiral or conventional two- and three-nucleon realistic potentials with the hyperspherical harmonics method, and electromagnetic currents derived in chiral effective field theory up to one loop. The predicted nd and $n{}^3\text{He}$ cross sections are in good agreement with data, but exhibit a significant dependence on the input Hamiltonian. A comparison is also made between these and new results for the nd and $n{}^3\text{He}$ cross sections obtained in the conventional framework for both potentials and currents.

PACS numbers: 13.40.-f, 21.10.Ky, 25.40.Lw

The nd and $n{}^3\text{He}$ radiative capture reactions at thermal neutron energy are very interesting, in that the magnetic dipole ($M1$) transitions connecting the continuum states to the hydrogen and helium bound states are inhibited at the one-body level. Hence, most of the calculated cross sections (80–90% in the case of $n{}^3\text{He}$) results from contributions of many-body components in the electromagnetic current operator [1]. Thus these processes provide a crucial testing ground for models describing these many-body operators and, indirectly, the nuclear potentials from which the ground- and scattering-state wave functions are derived.

Over the past two decades, chiral effective field theory (χEFT), originally proposed by Weinberg in a series of papers in the early nineties [2], has blossomed into a very active field of research. The chiral symmetry exhibited by quantum chromodynamics (QCD) severely restricts the form of the interactions of pions among themselves and with other particles. In particular, the pion couples to baryons, such as nucleons and Δ -isobars, by powers of its momentum Q , and the Lagrangian describing these interactions can be expanded in powers of Q/Λ_χ , where $\Lambda_\chi \sim 1$ GeV specifies the chiral-symmetry breaking scale. As a result, classes of Lagrangians emerge, each characterized by a given power of Q/Λ_χ and each involving a certain number of unknown coefficients, so called low-energy constants (LEC's), which are then determined by fits to experimental data (see, for example, the review papers [3] and [4], and references therein). Thus, χEFT provides, on the one hand, a direct connection between QCD and its symmetries, in particular chiral symmetry, and the strong and electroweak interactions in nuclei, and, on the other hand, a practical calculational scheme susceptible, in principle, of systematic improvement. In this sense, it can be justifiably argued to have put low-energy few-nucleon physics on a more fundamental basis.

Concurrent with these conceptual developments have been the acquisition and refinement of accurate meth-

ods for solving the $A=3$ and 4 Schrödinger equation (see Ref. [5] for a review). In this respect, it is worthwhile noting that the $A=4$ scattering problem has proven to be especially challenging for two reasons. The first is its coupled-channel nature: even at vanishing energies for the incident neutron, the elastic $n{}^3\text{He}$ and charge-exchange $p{}^3\text{H}$ channels are both open, and need to be accounted for. The second reason lies in the peculiarities of the ${}^4\text{He}$ spectrum, in particular the presence of resonant states between the $p{}^3\text{H}$ and $n{}^3\text{He}$ thresholds, which make it hard to obtain numerically converged solutions. Indeed, it is only very recently that both these capabilities have been fully realized [6, 7]. In the present work, the 3- and 4-body problems are solved with the hyperspherical-harmonics (HH) technique (see Ref. [8] for a review).

The developments outlined above make it possible to examine the question of whether available experimental data on these delicate processes—the nd and $n{}^3\text{He}$ captures—are well reproduced by theory. The present letter reports on such an effort by presenting results obtained both in χEFT as well as in the conventional framework based (essentially) on a meson-exchange model of potentials and electromagnetic current operators. This approach, while more phenomenological than χEFT , has a broader range of applicability, and accounts satisfactorily for a wide variety of nuclear properties and reactions up to energies, in some cases, beyond the pion production threshold, see Ref. [5] for a review. In particular, it reproduces well observed magnetic properties of $A = 2$ and 3 nuclei, including moments and form factors, as well as the np radiative capture, see Marcucci *et al.* (2005) [1].

The model for the nuclear electromagnetic current in χEFT up to one loop was derived originally by Park *et al.* [9], using covariant perturbation theory. In the last couple of years, two independent derivations, based on time-ordered perturbation theory (TOPT), have appeared in the literature, one by Kölling *et al.* [10] and the

other by some of the present authors [11]. There are technical differences in the implementation of TOPT, which relate to the treatment of reducible diagrams and are documented in considerable detail in the above papers. However, the resulting expressions in Refs. [10] and [11] for the two-pion-exchange currents (the only ones considered by the authors of Ref. [10]) are in agreement with each other, but differ from those of Ref. [9], in particular in the isospin structure of the $M1$ operator associated with

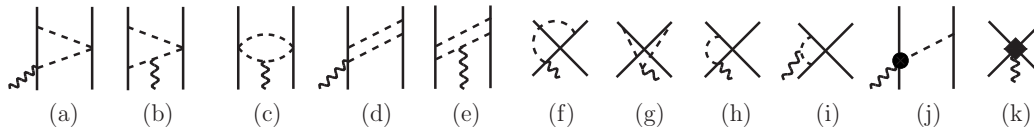


FIG. 1. Diagrams illustrating two-body currents at $N^3\text{LO}$. Nucleons, pions, and photons are denoted by solid, dashed, and wavy lines, respectively. Only one among the possible time orderings is shown for diagrams (a)-(j).

At $N^3\text{LO}$ (eQ) we distinguish three classes of terms [11]: i) two-pion exchange currents at one loop, illustrated by diagrams (a)-(i) in Fig. 1, ii) a tree-level one-pion exchange current involving the standard πNN vertex on one nucleon, and a $\gamma\pi NN$ vertex of order eQ^2 on the other nucleon, illustrated by diagram (j), and iii) currents generated by minimal substitution in the four-nucleon contact interactions involving two gradients of the nucleons' fields as well as by non-minimal couplings, collectively represented by diagram (k). A fourth class consisting of $(Q/m_N)^2$ relativistic corrections (RC's) to the NLO currents is neglected. However, RC's are not consistently treated in available chiral potentials, such as those employed below. For example, the RC's in the two-nucleon potential, implied by Poincaré covariance and just derived in Ref. [12] in an EFT context, have been omitted so far in $A=3$ and 4 calculations, even though their contribution is expected to be comparable to that of the three-nucleon potential [12].

The loop corrections in panels (a)-(i) involve the pion mass, the nucleon axial coupling constant $g_A=1.29$ (from the Goldberger-Treiman relation relating it to the πNN coupling constant), and the pion decay amplitude $F_\pi=184.8$ MeV. The LEC's entering panel (i) and the minimal currents in panel (k) have been determined by fits to the np S- and P-wave phase shifts up to 100 MeV laboratory energies [11]. We refer below to these constrained terms collectively as $N^3\text{LO(S-L)}$. There are five additional unknown LEC's: d'_8 , d'_9 , and d'_{21} in panel (j), and C'_{15} and C'_{16} in the non-minimal currents of panel (k). We denote these terms as $N^3\text{LO(LECs)}$ in the following. In a resonance saturation picture, the d'_8 and d'_{21} (d'_9) LEC's can be related to the combination of coupling constants and masses entering the isovector (isoscalar)

the one-loop corrections—see Pastore *et al.* (2009) [11] for a comparison and analysis of these differences.

Explicit expressions for the χEFT currents up to one loop, and associated $M1$ operators, are listed in Refs. [11]. Here we summarize succinctly their main features. The leading-order (LO) term results from the coupling of the external photon field to the individual nucleons, and is counted as eQ^{-2} (e is the electric charge). The NLO term (of order eQ^{-1}) involves seagull and in-flight contributions associated with one-pion exchange, and the $N^2\text{LO}$ term (of order eQ^0) represents the $(Q/m_N)^2$ relativistic correction to the LO one-body current (m_N denotes the nucleon mass).

$N-\Delta$ excitation and $\omega\pi\gamma$ ($\rho\pi\gamma$) transition currents [11]. Indeed, this connection is exploited in a series of calculations, based on the $M1$ operators derived in Ref. [9], of the np , nd , and $n^3\text{He}$ radiative captures, and magnetic moments of $A=2$ and 3 nuclei [9, 13]. Here, however, we adopt a different strategy, as discussed below. Lastly, we observe that at $N^3\text{LO}$ there are no three-body currents in the formalism of Ref. [11], which retains irreducible and recoil-corrected reducible diagrams.

The χEFT $M1$ operators have power-law behavior for large relative momenta k 's, and need to be regularized, before they can be inserted between nuclear wave functions. Following common practice, we implement this regularization by means of a cutoff $C_\Lambda(k) = \exp(-k^4/\Lambda^4)$, with Λ in the range (500–700) MeV, and constrain the LEC's entering the $N^3\text{LO}$ $M1$ operators of panels (j) and (k) in Fig. 1 to reproduce a set of observables for any given Λ in this range. This same renormalization procedure is adopted in the currently most advanced analyses of nuclear potentials, for example in Ref. [14] (see also Sec. II.C of Ref. [4], and references therein, for further discussion of this issue).

These operators are used in the present work to study the magnetic moments of the deuteron and trinucleons, and the np , nd , and $n^3\text{He}$ radiative captures at thermal neutron energies. The calculations are carried out by evaluating their matrix elements between wave functions obtained from either conventional or chiral (realistic) potentials with the variational HH method [8]. We consider the Argonne v_{18} [15] (AV18) and chiral $N^3\text{LO}$ [14] ($N^3\text{LO}$) two-nucleon potentials in combination with the Urbana-IX [16] (UIX) and chiral $N^2\text{LO}$ [17] ($N^2\text{LO}$) three-nucleon potentials. The AV18/UIX and $N^3\text{LO}/N^2\text{LO}$ Hamiltonians provide a very good descrip-

tion of three- and four-nucleon bound and scattering state properties, including binding energies, radii, and scattering lengths [7, 8].

We now turn our attention to the determination of the LEC's d'_8 , d'_9 , d'_{21} , C'_{15} , and C'_{16} . In principle, the d'_i could be fitted to pion photoproduction data on a single nucleon or, as mentioned already, related to hadronic coupling constants by resonance saturation arguments. Both procedures have drawbacks. While the former achieves consistency with the single-nucleon sector, it nevertheless relies on single-nucleon data involving photon energies much higher than those relevant to the threshold processes under consideration and real (in contrast to virtual) pions (some of these same issues in the context of three-nucleon potentials have been investigated in Ref. [18]). The second procedure is questionable because of poor knowledge of some of the hadronic couplings, such as $g_{\omega NN}$ and $g_{\rho NN}$.

Here, we assume $d'_{21}/d'_8 = 1/4$ as suggested by Δ -dominance, and rely on nuclear data to constrain the remaining four LEC's. The values obtained by reproducing the experimental np cross section and magnetic moments of the deuteron and trinucleons are listed in Table I. Note that the adimensional values reported there are in units of powers of Λ , *i.e.*, we have defined $d'_9 = d'_1/\Lambda^2$, $C'_{15} = d'_2/\Lambda^4$, $d'_{21} = d'_1/\Lambda^2$, and $C'_{16} = d'_2/\Lambda^4$ and the superscripts S and V denote the isoscalar and isovector content of the associated operators.

TABLE I. Adimensional values of the LEC's corresponding to cutoff parameters Λ in the range 500–700 MeV obtained for the AV18/UIX (N3LO/N2LO) Hamiltonian. See text for explanation.

Λ	$d'_1 \times 10^2$	d'_2	d'_1	d'_2
500	-8.85 (-0.225)	-3.18 (-2.38)	5.18 (5.82)	-11.3 (-11.4)
600	-2.90 (9.20)	-7.10 (-5.30)	6.55 (6.85)	-12.9 (-23.3)
700	6.64 (20.4)	-13.2 (-9.83)	8.24 (8.27)	-1.70 (-46.2)

In Fig. 2 we show results obtained by including cumulatively the contributions at LO, NLO, N²LO, and N³LO(S-L) for the deuteron (μ_d) and ³He/³H isoscalar (μ^S) magnetic moments (left panels), and for the np radiative capture cross section (σ_{np}^γ) at thermal energies and ³He/³H isovector (μ^V) magnetic moment (right panels). The NLO and N³LO(S-L) $M1$ operators are purely isovector, and hence do not contribute to μ_d and μ^S . The band represents the spread in the calculated values corresponding to the two Hamiltonian models considered here (AV18/UIX and N3LO/N2LO). The sensitivity to short-range mechanisms, encoded in the cutoff $C_\Lambda(k)$ and in the rather different short-range behaviors of the adopted potentials, remains quite weak for all these observables. Of course, taking into account the N³LO(LECs) contribution with the LEC values listed in Table I reproduces the experimental data represented by the black band (to accommodate errors, but these are negligible in the present case). The contributions at LO and NLO have the same

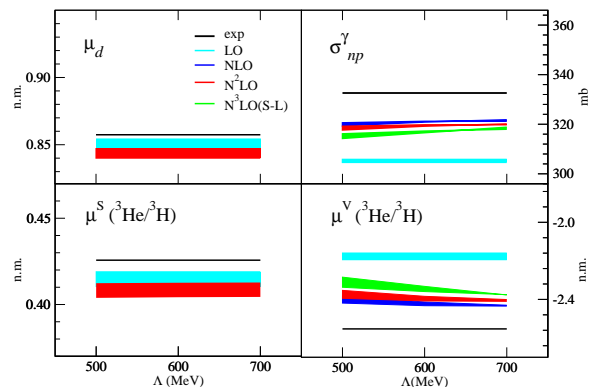


FIG. 2. Results for the deuteron and trinucleon isoscalar and isovector magnetic moments, and np radiative capture, obtained by including cumulatively the LO, NLO, N²LO, and N³LO(S-L) contributions. See text for discussion.

sign, while those at N²LO and N³LO(S-L) have each opposite sign, and tend to increase the difference between theory and experiment.

Having fully constrained the χ EFT $M1$ operator up to N³LO, we are now in a position to present predictions, shown in Fig. 3, for the nd and $n^3\text{He}$ radiative capture cross sections, denoted as σ_{nd}^γ and $\sigma_{n^3\text{He}}^\gamma$, and the photon circular polarization parameter R_c resulting from the capture of polarized neutrons on deuterons. The experimental data (black bands) are from Ref. [19] for nd and Ref. [20] for $n^3\text{He}$. Results obtained with the complete N³LO χ EFT operator are shown by the orange band labeled N³LO(LECs): those corresponding to the AV18/UIX (N3LO/N2LO) model delimit the upper (lower) end of the band in the case of nd , and its lower (upper) end in the case of $n^3\text{He}$. Their sensitivity to the cutoff, within a given model, is negligible for nd and at the 5–10% level for $n^3\text{He}$. The AV18/UIX and N3LO/N2LO results are within $\simeq 2\%$ of the nd experimental cross section. However, at $\Lambda=600$ MeV, for example, the experimental $\sigma_{n^3\text{He}}^\gamma$ is well reproduced in the N3LO/N2LO calculation, but underpredicted by $\simeq 15\%$ in the AV18/UIX. As expected, these processes are strongly suppressed at LO: the calculated $\sigma_{nd}^\gamma(\text{LO})$ and $\sigma_{n^3\text{He}}^\gamma(\text{LO})$ are less than half and a factor of five smaller than the measured values. In the case of $n^3\text{He}$, the matrix element at NLO is of opposite sign and twice as large (in magnitude) compared to that at LO, hence $\sigma_{n^3\text{He}}^\gamma(\text{LO})$ and $\sigma_{n^3\text{He}}^\gamma(\text{LO} + \text{NLO})$ are about the same, as seen in Fig. 3. For nd , however, the LO and NLO contributions interfere constructively. For both nd and $n^3\text{He}$, the N²LO and N³LO(S-L) corrections exhibit the same pattern discussed in connection with Fig. 2. The N³LO(LECs) contributions are large, and essential for bringing theory into good agreement with experiment.

In Fig. 3 we also show results obtained in the conventional framework, referred to as the standard nuclear physics approach (SNPA), with the AV18/UIX Hamiltonian model. The electromagnetic current operator in-

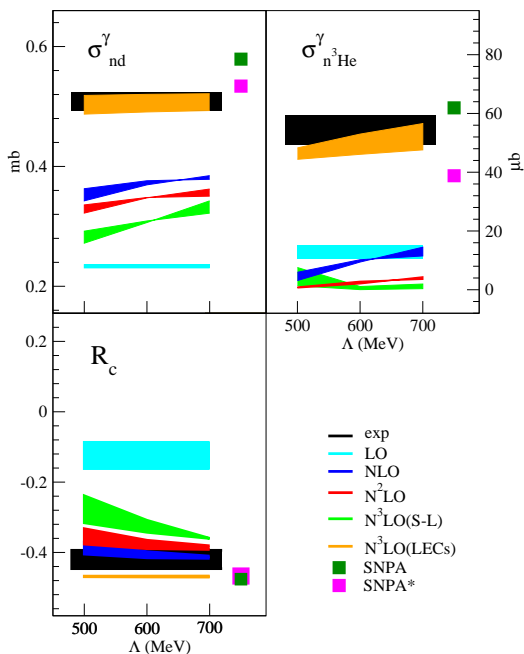


FIG. 3. Results for σ_{nd}^γ (left top panel), $\sigma_{n^3\text{He}}^\gamma$ (right top panel), and R_c (left bottom panel), obtained by including cumulatively the LO, NLO, N²LO, N³LO(S-L), and N³LO(LECs) contributions. Also shown are predictions obtained in the standard nuclear physics approach (squares labeled SNPA and SNPA*). See text for discussion.

cludes the one-body term—the same as the χ EFT LO operator discussed earlier—as well as two- and three-body terms, constructed from the two- and three-nucleon potentials (AV18 and UIX, respectively) so as to satisfy exactly current conservation with them, see Marcucci *et al.* (2005) [1]. In the figure, the squares labeled SNPA* represent the results obtained by retaining in addition the relativistic corrections to the one-body current (*i.e.*, the χ EFT N²LO operator). These corrections had been neglected in all previous studies of these processes [1]. In fact, their contributions are found to be numerically significant and, at least for the case of nd capture, bring the present SNPA* results within $\simeq 4\%$ and 2% , respectively, of the experimental data and χ EFT predictions (based on the AV18/UIX model). However, it should be emphasized that the SNPA (and SNPA*) currents contain no free parameters—*i.e.*, they are not constrained to fit any photonuclear data, in contrast to the χ EFT currents. From this perspective, the achieved level of agreement between SNPA* and data should be viewed as satisfactory, especially when considering, in the χ EFT context, the large role played by the N³LO(LECs) currents.

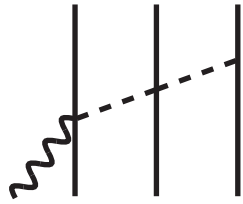
We conclude by remarking that the convergence of the chiral expansion is problematic for these processes. The LO is unnaturally small, since the associated operator cannot connect the dominant S-states in the hydrogen and helium bound states (in contrast to np capture, for example) [1]. This leads to an enhancement of the NLO, which, however, in the case of $n^3\text{He}$ is offset by the de-

structive (and accidental) interference between it and the LO contribution. It appears that at N⁴LO no additional LEC’s enter, Park *et al.* (2000) [13]. Thus, inclusion of the N⁴LO currents would have to be followed by a “rescaling” of the LEC’s in Table I, in order to reproduce (as before at N³LO) the experimental values of μ_d , $\mu^{S,V}$, and σ_{np}^γ . The resulting predictions for σ_{nd}^γ and $\sigma_{n^3\text{He}}^\gamma$ would presumably be close to those obtained here at N³LO.

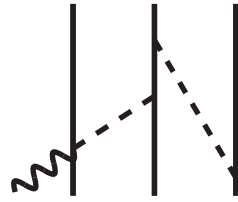
It is likely that explicit inclusion of Δ degrees of freedom would significantly improve the convergence pattern, particularly in view of the relevance of the pion-exchange current of panel (j) in Fig. 1—in such a theory, this operator would be promoted to N²LO [11]. We plan to pursue vigorously this line of research in the future.

The work of R.S. is supported by the U.S. Department of Energy, Office of Nuclear Physics under contract DE-AC05-06OR23177.

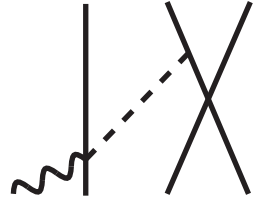
- [1] J.L. Friar, B.F. Gibson, and G.L. Payne, Phys. Lett. **B251**, 11 (1990); R. Schiavilla *et al.*, Phys. Rev. C **45**, 2628 (1992); M. Viviani, R. Schiavilla, and A. Kievsky, Phys. Rev. C **54**, 534 (1996); L.E. Marcucci *et al.* Phys. Rev. C **72**, 014001 (2005).
- [2] S. Weinberg, Phys. Lett. **B251**, 288 (1990); Nucl. Phys. **B363**, 3 (1991); Phys. Lett. **B295**, 114 (1992).
- [3] P.F. Bedaque and U. van Kolck, Ann. Rev. Nucl. Part. Sci. **52**, 339 (2002).
- [4] E. Epelbaum, H.W. Hammer, and U.-G. Meissner, Rev. Mod. Phys. **81**, 1773 (2009).
- [5] J. Carlson and R. Schiavilla, Rev. Mod. Phys. **70**, 743 (1998).
- [6] A. Deltuva and A.C. Fonseca, Phys. Rev. C **76**, 021001; R. Lazauskas, Phys. Rev. C **79**, 054007 (2009).
- [7] M. Viviani *et al.*, arXiv:1007.2052, Phys. Rev. C in press.
- [8] A. Kievsky *et al.*, J. Phys. **G35**, 063101 (2008).
- [9] T.-S. Park, D.-P. Min, and M. Rho, Nucl. Phys. **A596**, 515 (1996).
- [10] S. Kölling *et al.*, Phys. Rev. C **80**, 045502 (2009).
- [11] S. Pastore, R. Schiavilla, and J.L. Goity, Phys. Rev. C **78**, 064002 (2008); S. Pastore *et al.*, Phys. Rev. C **80**, 034004 (2009).
- [12] L. Girlanda *et al.*, Phys. Rev. C **81**, 034005 (2010).
- [13] T.-S. Park *et al.*, Phys. Lett. **B472**, 232 (2000); Y.-H. Song *et al.*, Phys. Lett. **B656**, 174 (2007); Y.-H. Song, R. Lazauskas, and T.-S. Park, Phys. Rev. C **79**, 064002 (2009); R. Lazauskas, Y.-H. Song, and T.-S. Park, arXiv:0905.3119.
- [14] D.R. Entem and R. Machleidt, Phys. Rev. C **68**, 041001 (2003).
- [15] R.B. Wiringa, V.G.J. Stoks, and R. Schiavilla, Phys. Rev. C **51**, 38 (1995).
- [16] B.S. Pudliner *et al.*, Phys. Rev. C **56**, 1720 (1997).
- [17] D. Gazit, S. Quaglioni, and P. Navratil, Phys. Rev. Lett. **103**, 102502 (2009).
- [18] V.R. Pandharipande, D.R. Phillips, and U. van Kolk, Phys. Rev. C **71**, 064002 (2005).
- [19] E.T. Jurney, P.J. Bendt, and J.C. Browne, Phys. Rev. C **25**, 2810 (1982); M.W. Konijnenberg *et al.*, Phys. Lett. **B205**, 215 (1988).
- [20] F.L.H. Wolfs *et al.*, Phys. Rev. Lett. **63**, 2721 (1989); R. Wervelman *et al.*, Nucl. Phys. **A526**, 265 (1991).



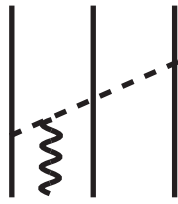
(a)



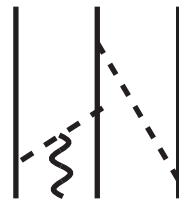
(b)



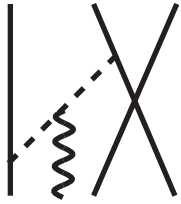
(c)



(d)



(e)



(f)